eprints@whiterose.ac.uk
https://eprints.whiterose.ac.uk/

On the use of hot-spot stresses, effective notch stresses and the Point Method to estimate lifetime of inclined welds subjected to uniaxial fatigue loading

Ibrahim Al Zamzami and **Luca Susmel**

Department of Civil and Structural Engineering, The University of Sheffield,
Mappin Street, Sheffield S1 3JD, United Kingdom

<u>Corresponding Author</u>:   Prof. **Luca Susmel**
Department of Civil and Structural Engineering
The University of Sheffield, Mappin Street, Sheffield, S1 3JD, UK
Telephone: +44 (0) 114 222 5073
Fax: +44 (0) 114 222 5700
E-mail: l.susmel@sheffield.ac.uk

ABSTRACT

The present paper addresses the problem of estimating fatigue strength of welded joints when the weld seams are inclined with respect to the direction of the axial cyclic loading being applied. From a fatigue design point of view, the main complexity lies in the fact that, with this particular welded geometries, although the applied loading is uniaxial, accurate fatigue assessment can be performed provided that the degree of multiaxiality of the nominal/structural/local stress states at the weld toes/roots is modelled effectively. To this end, in the present investigation the Modified Wöhler Curve Method (MWCM) is attempted to be used to assess the fatigue strength of steel joints with inclined welds by using this multiaxial fatigue criterion in conjunction with nominal stresses, hot-spot stresses, effective notch stresses, and the Theory of Critical Distances (TCD). A large number of experimental results taken from the literature and generated by testing inclined fillet welds was used to check the accuracy and reliability of the MWCM applied along with these different ways of determining the relevant stress states. The results obtained from this validation exercise demonstrate that the MWCM returns satisfactory estimates when it is used to assess fatigue strength in the presence of inclined welds, with this holding true independently of the specific stress analysis strategy being adopted.

Keywords: Inclined welds, nominal stress, hot-spot stress, local stress, critical distance.

Nomenclature

a, b, α, β	fatigue constants for the MWCM's calibration curves
k	negative inverse slope of the uniaxial fatigue curve
k_0	negative inverse slope of the torsional fatigue curve
k_τ	negative inverse slope of the modified Wöhler curve
P_S	probability of survival
$\Delta\sigma_x$	stress range normal to the weld seam
$\Delta\sigma_{nom}$	axial nominal stress range
$\Delta\sigma_n$	stress range perpendicular to the critical plane
$\Delta\sigma_A$	stress range of the uniaxial design curve extrapolated at a reference number of cycles to failure
$\Delta\sigma_{0.4t}$	normal superficial stress range at a distance from the weld toe equal to 0.4t
$\Delta\sigma_t$	superficial normal stress range at a distance from the weld toe equal to t
$\Delta\sigma_{R,d}, \Delta\tau_{R,d}$	design resistance stress range for a specific number of cycles and appropriate FAT class
$\Delta\tau_{xy}$	shear stress range parallel to the weld seam
$\Delta\tau$	shear stress range relative to the critical plane
$\Delta\tau_{0.4t}$	superficial shear stress range at a distance from the weld toe equal to 0.4t
$\Delta\tau_t$	superficial shear stress range at a distance from the weld toe equal to t
$\Delta\tau_A$	stress range of the torsional design curve extrapolated at a reference number of cycles to failure
ρ_w	critical plane stress ratio
$\Delta\tau_{Ref}$	reference shear stress range extrapolated at N_{Ref} cycles to failure
N_{Ref}	reference number of cycles to failure
N_f	number of cycles to failure
r_{Ref}	reference radius
θ	inclination angle with respect to the applied cyclic loading
R	load ratio

1. Introduction

Failure of metals caused by cyclic loading is a very complex problem that has been investigated extensively since the second half of the 19th century. Damage due to fatigue is accumulated cycle by cycle until, after a certain number of cycles, materials fail suddenly without any visible warning [1-3]. In this general context, a considerable amount of research work has been carried out since the beginning of the last century to investigate the effect of welding processes on the overall fatigue behaviour of structural components. These studies indicate that the fatigue strength of welded components is considerably lower than the one of un-welded structural details, with this holding true even though they are made of the same material [1].

2

This is a consequence of the fact that residual stresses, defects, imperfections and distortions are introduced during welding, with this resulting in an intrinsic reduction of the overall fatigue strength of welded connections [2, 4, 5]. Further, localised stress concentration phenomena resulting in severe stress/strain gradients always occur at the weld toes as well as at the weld roots [6]. This is the reason why fatigue cracks in welded joints usually initiate in the vicinity of the weld seams rather than in the parent material [2]. This already complex situation is further complicated also by the fact that in the heat affected zone the filler material alters the metallurgical morphology of the parent material, with this leading to a change in the material microstructural features in the vicinity of the welds themselves [2].

Owing to the key role that is played by weldments in applications of industrial interest (such as, for instance, automotive, offshore structures and railway industry), a considerable amount of experimental/theoretical work has been done to formalise and validate specific design techniques suitable for performing fatigue assessment of structural welded components [7-9]. As a result, the available Standards and Codes of Practice suggest different design strategies that include the nominal stress approach, the hot-spot stress approach, and those methods making use of local stresses [9-11]. In this context, certainly, the nominal stress approach is the most widely used in situations of practical interest. In particular, according to this methodology, fatigue strength is directly estimated from *ad hoc* S-N curves that are provided, for specific welded geometries, by the pertinent Standard Codes. To perform fatigue assessment according to this approach the stress analysis is done according to the simple principles of continuum mechanics [9-12]. Even if it is very effective, the main limitation characterising the nominal stress approach is that it cannot be used either when there is no univocal nominal cross-section or when a reference design curve is not available for the specific welded geometry being designed [13]. As the nominal stress approach is not directly applicable, then either hot-spot stresses or local stresses have to be employed to design against fatigue complex/non-standard welded geometries.

The hot-spot stress approach works by taking into account the stress raising effect by extrapolating a reference stress quantity at the weld toes, with the stress gradient effect being accounted for via *ad hoc* design curves [13, 14].

Even if hot-spot stresses have proven to be very effective, examination of the state of the art shows that the most advanced design approaches available to date are those making use of local linear-elastic stresses. In this context, the so-called effective notch stress approach [14-18] is the most advanced fatigue design method being recommended by the International Institute of Welding (IIW) [9]. According to this approach, design stresses are determined by rounding weld toes/roots with a fictitious notch radius equal to either 1 mm (when the thickness, t, is larger than 5 mm) or to 0.05 mm (for t<5 mm) [16-18].

More recently, attention has been focused on extending the use of the Theory of Critical Distance (TCD) [19] also to the fatigue assessment of weldments [20]. The TCD takes as a starting point the idea that fatigue damage in the presence of stress concentrators of all kinds can be estimated by using an effective stress that is representative of the entire linear-elastic stress field acting on the material in the vicinity of the assumed crack initiation locations [21]. Thanks to its unique features, the TCD is seen to return very accurate estimates of the fatigue lifetime of welded components, the key advantage being that the required stress fields can be determined directly from simple linear-elastic Finite Element (FE) models [12, 19-21].

The available Design Codes [9-11] recommend specific design rules that can be used primarily in those situations where the cyclic force being applied is either normal or parallel to the weld seams. However, this is not always the case. In fact, in real welded structures, in-service forces can be applied also at different angles to the weld seams. To address this type of design problem, Eurocode 3 [10] and Eurocode 9 [11] suggest to estimate fatigue damaged by considering the effect of the stress ranges that are both normal and parallel to the weld toe. Similarly, to address this specific problem, the IIW [9] recommends using a relationship that is directly derived from the classic equation due to Gough, i.e.:

$$\left(\frac{\Delta\sigma_{eq,S,d}}{\Delta\sigma_{R,d}}\right)^2 + \left(\frac{\Delta\tau_{eq,S,d}}{\Delta\tau_{R,d}}\right)^2 \leq CV \tag{1}$$

In Eq. (1), $\Delta\sigma_{eq,S,d}$ and $\Delta\tau_{eq,S,d}$ are equivalent constant amplitude stress ranges, whereas $\Delta\sigma_{R,d}$ and $\Delta\tau_{R,d}$ are design stress ranges for a specific number of cycles estimated from appropriate uniaxial and torsional FAT curves. Finally, CV is a reference comparison index that is directly provided in Ref. [9].

Turning to the research work that has been done to address the problem of designing against fatigue uniaxially loaded inclined welds, recently, we have proposed a simple formula that was derived by tackling the problem from a multiaxial fatigue angle [22]. In particular, we obtained very accurate estimates by simply applying the Modified Wöhler Curve Method (MWCM) [11, 23-26] along with the nominal stresses approach [27]. In light of the high level of accuracy that was obtained by employing this strategy, the ultimate goal of this paper is assessing the accuracy of the MWCM in estimating fatigue strength in the presence of uniaxially loaded inclined welds when our multiaxial fatigue criterion is applied along with hot-spot and effective notch stresses as well as in conjunction with the Point Method (PM) – i.e., the simplest formalisation of the TCD [11, 21].

2. Fundamental features of the MWCM

Examination of the state of the art shows that the MWCM is one of the most advanced tools that can be used to assess the strength of welded components subjected to multiaxial fatigue loading. In particular, this method – that can be applied in terms of either nominal, hot-spot or local stresses - has proven to be highly accurate and reliable in estimating lifetime of steel and aluminium welded joints subjected to in-phase/out-of-phase constant/variable amplitude uniaxial/multiaxial fatigue loading [27-36].

The procedure to design welded joints against fatigue according to the MWCM is summarised in Figs 1 and 2, with this general theoretical framework being valid independently of the type of stresses being used (i.e., either nominal, hot-spot, or local stresses). Initially, the hypothesis

is formed that the welded component being designed is subjected to a cyclic load history that results in a multiaxial stress state, $[\Delta\sigma]$, at the critical location/section. Stress tensor $[\Delta\sigma]$ is then post-process to calculate the shear stress range, $\Delta\tau$, and the normal stress range, $\Delta\sigma_n$, relative to that material plane experiencing the maximum shear stress range (i.e., the so called critical plane) [36, 37].

The MWCM takes into account the combined effect of $\Delta\tau$ and $\Delta\sigma_n$ through a stress ratio, ρ_w, which is the defined as follows (Eq.2) [12, 27]:

$$\rho_w = \frac{\Delta\sigma_n}{\Delta\tau} \tag{2}$$

According to the way it is defined, stress ratio ρ_w is sensitive to the degree of multiaxiality and non-proportionality of the assessed cyclic load history [12, 36]. In particular, it is straightforward to see that ρ_w is invariably equal to unity under fully-reversed axial cyclic loading and invariably equal to zero under pure torsional fatigue loading [12].

In order to explain how the MWCM works, consider the maximum shear stress range, $\Delta\tau$, vs. number of cycles to failure, N_f, diagram that is reported in Fig. 3 (which is usually referred to as the "modified Wöhler diagram"). According to this log-log schematisation, welded components are designed using a modified Wöhler curve whose position varies as ratio ρ_w changes. Any of these design curves is defined unambiguously via its negative inverse slope, $k_\tau(\rho_w)$, and its endurance limit, $\Delta\tau_{Ref}(\rho_w)$, extrapolated at N_{Ref} cycles to failure. The schematic diagram of Fig. 3 makes it evident that fatigue lifetime can be assessed provided that the specific modified Wöhler curve is known for the value of ρ_w calculated, according to Eq. (2), by post-processing the load history under investigation. Since the S-N curves that are available to perform the fatigue assessment are usually those experimentally determined/estimated under fully-reversed uniaxial and torsional fatigue loading, the modified Wöhler curves for ρ_w ratios different from unity (uniaxial case) and zero (torsional case) have to be derived via the following linear relationships [12, 23, 24]:

$$k_\tau(\rho_w) = \alpha \cdot \rho_w + \beta \qquad (3)$$

$$\Delta\tau_{Ref}(\rho_w) = a \cdot \rho_w + b \qquad (4)$$

In Eqs (3) and (4) α, β, a and b are fatigue constants to be determined from suitable experimental fatigue curves. In particular, by observing that $\rho_w = 1$ under fully-reversed uniaxial cyclic loading and $\rho_w = 0$ under torsional fatigue loading, Eqs (3) and (4) can directly be rewritten as follows [12, 24]:

$$k_\tau(\rho_w) = (k - k_0) \cdot \rho_w + k_0 \qquad (5)$$

$$\Delta\tau_{Ref}(\rho_w) = \left(\frac{\Delta\sigma_A}{2} - \Delta\tau_A\right) \cdot \rho_w + \Delta\tau_A \qquad (6)$$

where k and k_0 are the negative inverse slopes of the uniaxial and torsional fatigue curve, respectively, whereas $\Delta\sigma_A$ and $\Delta\tau_A$ are the ranges of the corresponding endurance limits determined at a number of cycles to failure equal to at N_{Ref}.

Turning back to the way the MWCM quantifies fatigue damage, after using Eqs (5) and (6) to estimate the modified Wöhler curve associated with the value of ρ_w characterising the load history under investigation, the number of cycles to failure can be predicted directly via the following standard power law (Fig. 3):

$$N_f = N_{Ref} \cdot \left[\frac{\Delta\tau_{Ref}(\rho_w)}{\Delta\tau}\right]^{k_\tau(\rho_w)} \qquad (7)$$

To conclude, it is worth recalling here that, according to the way it is defined, ratio ρ_w is not sensitive to presence of non-zero mean stress [12, 27, 36]. This implies that the MWCM as reviewed in the present section can be used to perform the fatigue assessment of welded joints characterised by high tensile residual stresses – i.e., in the as-welded condition. In contrast,

the fatigue assessment of stress-relieved welded connections is recommended to be performed by adopting appropriate enhancement factors as extensively discussed in Ref. [36].

3. Experimental data taken from the technical literature

To assess the accuracy of the MWCM in estimating the fatigue strength of inclined welds, a number of experimental data sets were selected from the technical literature. These results were generated by testing under zero-tension (i.e., R=0) uniaxial cyclic loading steel specimens manufactured by making the weld inclination angle, θ, vary in the range 0°-45°. In particular, we considered the welded specimens tested by Booth and Maddox (Fig. 4a) [38], the load-carrying fillet welded joints tested by Kim and Kainuma (Fig .4b) [39] and the out-of-plane gusset geometry (Fig. 5a) as well as the non-load carrying fillet welded joint (Fig. 5b) tested by Kim and Yamada [40].

These welded specimens were all in the as-welded condition, i.e., no heat treatment was used to relieve the internal residual stresses arising from the welding process.

After welding, all the samples were mechanically treated to force the fatigue cracks to initiate at the middle section of the weld seams (either at the weld toes or at the weld roots). In particular, the out-of-plane gusset specimens (specimen type KY-G in Fig. 5a [40]) were either grounded with a disc grinder or needle peened to ensure that the fatigue cracking process did not occur at the weld edges. The length of the gusset was fixed so that the distance between the end of the gusset and the edge of the specimen was 20 mm. Accordingly, the gusset length varied with inclination angle θ. For the non-load carrying fillet (specimen type KY-N in Fig. 5b [40]), the two stiffeners and the area in between were widened with a fillet radius equal to 15 mm to reduce the stress concentration effect and ensure no fatigue cracks initiated at the edges. For the load-carrying fillet welded joints (specimen type KK in Fig. 4b [39]), the root gap was less than 0.1 mm and the specimens were grounded with a disc grinder at the weld toe to prevent fatigue failures to occur in these locations.

Finally, it is worth observing that the welded geometries sketched in Figs 4 and 5 were used to check the accuracy of the MWCM when this approach is applied in terms of nominal and

effective notch stress as well as in conjunction with the TCD. The hot-spot stress approach was used instead solely to post-process the results generated by testing the welded specimens shown in Figs. 4a, 5a and 5b. This is due to the fact that in the load-carrying fillet welded joints tested by Kim and Kainuma (Fig .4b) [39] fatigue cracks were seen to initiate from the weld roots and the hot-spot stress approach cannot be used to assess this type of failure [13, 14].

4. Inclined welds, nominal Stresses and the MWCM: a brief review

The nominal stress approach is the simplest design technique that is suggested both by the European Standard Codes [10, 11] and by the IIW [9]. According to this approach, design stresses are calculated using classic continuum mechanics by considering, where necessary, the macroscopic stress gradients resulting from the macro-geometrical features characterising the weld regions [9, 12]. In contrast, local stress concentration phenomena due to the weld seams are neglected since their detrimental effect is directly taken into account via the specific design fatigue curve that is recommended for each welded geometry being classified [9-11].

Back in 2004 the MWCM applied in terms of nominal stresses was seen to be highly accurate in estimating fatigue lifetime of aluminium and steel welded joints when the loads are applied parallel and perpendicular to the weld seams [12, 27, 32, 36]. Recently, the combined use of the MWCM and the nominal stress approach was extended also to the fatigue assessment of uniaxially loaded inclined welds [22]. For these welded geometries, although the global load history is uniaxial, the nominal stress state in the vicinity of the weld is not only multiaxial, but also varies proportionally, with the degree of proportionality changing as the weld inclination angle increases [22].

According to the sketch reported in Fig. 6a, the nominal stresses perpendicular, $\Delta\sigma_x$, and parallel, $\Delta\tau_{xy}$, to the weld seam can easily be determined as follows [41]:

$$\Delta\sigma_x = \Delta\sigma_{nom} \cdot cos^2\theta \tag{8}$$

$$\Delta\tau_{xy} = \Delta\sigma_{nom} \cdot cos\theta \cdot sin\theta \tag{9}$$

where θ is the angle between the weld seam and the straight line normal to the direction along which the cyclic uniaxial force is applied (Fig. 6a). The use of the nominal stresses determined according to Eqs (8) and (9) to estimate the fatigue strength of welded joints can be justified by advocating the Notch-Stress Intensity Factor (N-SIF) approach [42, 43]. In particular, for a notch opening angle larger than 100°, Mode II stresses are no longer singular, so that they can be neglected with little loss of accuracy. In contrast, the overall fatigue strength of welded joints is seen to depend predominantly on the Mode I and Mode III stress components, with the corresponding linear-elastic stress fields being still singular also for weld opening angles equal to 135° [43, 44]. Since, Mode I and Mode III stresses are proportional to nominal stresses $\Delta\sigma_x$ and $\Delta\tau_{xy}$, respectively, the stress quantities determined according to Eqs (8) and (9) can directly be used to assess fatigue strength when the weld seams are subjected to a multiaxial system of normal and shear forces [22, 44].

Having clarified this important aspect, as per the schematic Mohr circle reported in Fig.6b, the ranges of the normal and shear nominal stress relative to the critical plane can then be determined as [22]:

$$\Delta\sigma_n = \frac{\Delta\sigma_x}{2} = \frac{\Delta\sigma_{nom}}{2} \cdot cos^2\theta \tag{10}$$

$$\Delta\tau = \sqrt{\frac{\Delta\sigma_x^2}{4} + \Delta\tau_{xy}^2} = \frac{\Delta\sigma_{nom}}{2} \cdot cos^2\theta\sqrt{1 + 4tan^2\theta} \text{ for } \theta \neq \frac{\pi}{2} \tag{11}$$

If q is used to define the following trigonometric quantity:

$$q = \frac{1}{\sqrt{1+4tan^2\theta}} \tag{12}$$

then the critical plane stress ratio, Eq. (2), can directly be determined as:

$$\rho_w = \frac{\Delta\sigma_n}{\Delta\tau} = \frac{1}{\sqrt{1+4tan^2\theta}} = q \tag{13}$$

Eq. (13) makes it evident that, as far as uniaxially loaded inclined welds are concerned, ρ_w depends solely on the inclination angle, θ. Since $\rho_w = q$, then the MWCM's calibration equations – i.e., Eqs (5) and (6), can then be rewritten as [22]:

$$k_\tau(\rho_w) = k_\tau(q) = (k - k_0) \cdot q + k_0 \tag{14}$$

$$\Delta\tau_{Ref}(\rho_w) = \Delta\tau_{Ref}(q) = \left(\frac{\Delta\sigma_A}{2} - \Delta\tau_A\right) \cdot q + \Delta\tau_A \tag{15}$$

Finally, according to Eq. (7), the number of cycles to failure can be estimated via the following relationship:

$$N_f = N_{Ref} \cdot \left[q \cdot \frac{q\Delta\sigma_A + 2\Delta\tau_A(1-q)}{\Delta\sigma_{nom} \cdot \cos^2\theta}\right]^{(k-k_0)\cdot q + k_0} \tag{16}$$

To check the overall level of accuracy that is obtained by applying the MWCM along with the nominal stress approach, Eqs (14) and (15) were calibrated as described in what follows.

As far as non-loading transverse fillet-welded joints are concerned, the IIW [9] recommends using uniaxial and torsional fatigue curves having endurance limits $\Delta\sigma_A$ and $\Delta\tau_A$ (extrapolated at N_{Ref} =2·10⁶ cycles to failure and determined for a probability of survival, P_S, of 97.7%) equal to 71 MPa (with k=3) and 80 MPa (with k_0=5), respectively. The $\Delta\sigma_{nom}$ vs. N_f log-log diagram of Fig. 7a confirms that the FAT 71 curve was capable of accurately modelling the fatigue behaviour of the θ=0° configurations for specimens BM (Fig. 4a), KY-G (Fig. 5a), and KY-N (Fig. 5b).

When cracks emanate from the weld roots - as it was observed in the KK specimens (Fig. 4b) [39], the IIW suggests using instead a uniaxial fatigue curve having $\Delta\sigma_A$ =36 MPa (at N_{Ref} =2·10⁶ cycles to failure) with k=3 and a torsional design curve having $\Delta\tau_A$ =80 MPa (at N_{Ref} =2·10⁶ cycles to failure) and k_0=5. As expected, the chart of Fig. 7b fully confirms that the FAT 36 design curve was suitable for modelling the fatigue strength of the KK specimens (Fig.

4b), i.e., for assessing those situations where final breakage took place as a result of weld root cracking.

It is possible to conclude by observing that the modified Wöhler diagrams of Fig. 8 (see also Table 1) confirm that the MWCM applied in conjunction with the nominal stress approach is highly accurate in assessing the extent of fatigue damage in the presence of uniaxially loaded inclined welds, with this holding true independently of the type of failure (i.e., either toe or root cracking). In particular, the obtained level of accuracy is certainly satisfactory because the experimental results are seen to fall within error bands being characterised by a scatter ratio of the reference stress range for P_S=97.7%/2.3% equal to 1.85 [34]. This value for the scatter ratio was recalculated from the reference value of 1.5 suggested by Haibach [45] for P_S=90%/10% and determined by reanalysing a large number of experimental results obtained under uniaxial fatigue loading from different welded geometries. We recalculated the scatter ratio for P_S=97.7%/2.3% because Eurocode 3 recommends to perform the fatigue assessment of welded joints by always referring to design fatigue curves determined for a probability of survival, P_S, equal to at least 97.7% [10]. The fact that our estimates fall within Haibach's normalised scatter bands (Fig. 8) fully confirms the statistical significance of the obtained results. This strategy based on Haibach's reference scatter ratio will be used in what follows also to assess the accuracy of the MWCM applied along with hot-spot and local stresses.

5. Accuracy of the MWCM applied along with the hot-spot stress approach

The hot-spot stress approach takes as its starting point the idea that fatigue design stresses can be extrapolated directly at the weld toe from a linear stress distribution obtained by interpolating the stress states at two or three superficial reference points (see also Fig. 1b). These reference stress states are usually determined either by using strain gauges or by solving linear-elastic FE models with mesh size set according to specific geometrical rules [9, 14]. When the FE method is used, hot-spot stresses can be determined either via surface stress extrapolation or via through-thickness stress linearization [9, 46].

To check the accuracy of the MWCM applied along with the hot-spot stress approach in estimating fatigue lifetime of uniaxially loaded inclined welds, the hot-spot stress components parallel, $\Delta\tau_{HS}$, and perpendicular, $\Delta\sigma_{HS}$, to the weld seam (Fig. 1b) [12, 28] were determined using the surface extrapolation method [9] as follows:

$$\Delta\sigma_{HS} = 1.67\Delta\sigma_{0.4t} - 0.67\Delta\sigma_t \tag{17}$$

$$\Delta\tau_{HS} = 1.67\Delta\tau_{0.4t} - 0.67\Delta\tau_t \tag{18}$$

In more detail, according to Fig. 1, stress components $\Delta\sigma_{0.4t}$ and $\Delta\tau_{0.4t}$ were determined at a distance from the weld toe equal to 0.4t (with t being the thickness), whereas stress components $\Delta\sigma_t$ and $\Delta\tau_t$ at a distance from the weld toe equal to t. This was done by using commercial FE code ANSYS® to solve three-dimensional linear-elastic FE models where the mesh density was set according to the IIW recommendations [9, 34] (see the example shown in Fig. 9).

The MWCM's governing equations, Eqs (5) and (6), were calibrated using the FAT 100 uniaxial fatigue curve ($\Delta\sigma_A$ =100 MPa at N_{Ref} = 2·10[6] cycles to failure for P_S=97.7% and k=3) and the FAT 80 torsional fatigue curve ($\Delta\tau_A$ =80 MPa at N_{Ref} = 2·10[6] cycles to failure for P_S=97.7% and k_0=5) [9], obtaining:

$$k_t(\rho_w) = -2 \cdot \rho_w + 5 \tag{19}$$

$$\Delta\tau_{Ref}(\rho_w) = -47.5 \cdot \rho_w + 80 \; [\text{MPa}] \tag{20}$$

As far as weld toe failures are concerned, the $\Delta\sigma_{HS}$ vs. N_f log-log diagram of Fig. 7c makes it evident that the use of the FAT 100 uniaxial fatigue curve recommended by the IIW [9] to assess (in terms of hot-spot stresses) the fatigue strength of the considered θ=0° welded specimens resulted in slightly non-conservative estimates.

The overall accuracy we obtained by applying the MWCM in conjunction with the hot-spot stress approach to estimate the fatigue strength of welded geometries BM (Fig. 4a), KY-N (Fig. 5a), and KY-G (Fig. 5b) is shown in the modified Wöhler diagrams of Fig. 10 (see also Table 1). These charts make it evident that the MWCM returns accurate predictions also when it is applied along with the hot-spot approach, the obtained level of conservatism slightly increasing as the inclination angle, θ, increases.

6. Accuracy of the MWCM applied along with the effective notch stress approach

By taking full advantage of Neuber's micro-support theory [13, 47], the effective notch stress approach [13, 15] estimates the fatigue strength of welded components via the local linear-elastic stresses that are determined by rounding weld toes and roots (Fig. 2a). When the thickness of the welded connections being designed is larger than 5 mm, then design stresses are recommended to be determined by using a weld toe/root fictitious radius, r_{ref}, equal to 1 mm [9, 18]. In contrast, when the main plate thickness is lower than 5 mm, weld toes and roots have to be rounded by using a fictitious radius of 0.05 mm [18].

Since all the welded joints considered in the present investigation had thickness larger than 5 mm, notch stresses were determined using FE code ANSYS® by rounding the weld toes of specimens BM (Fig. 4a), KY-G (Fig. 5a), and KY-N (Fig. 5b) and the weld roots of specimens KK (Fig. 4b) by setting r_{ref} invariably equal to 1 mm. The stress analysis was performed via three-dimensional FE models solved by following a conventional solid-to-solid sub-modelling procedure, with the mesh density being gradually increased until convergence occurred (see the example shown in Fig. 9).

The MWCM was applied along with the reference radius concept [34] by calibrating its governing equations, Eqs (5) and (6), using the FAT 225 uniaxial fatigue curve [9, 18] and the FAT 160 torsional fatigue curve [18]. In more detail, the uniaxial calibration curve had endurance limit, $\Delta\sigma_A$, extrapolated at N_{Ref} = 2·10⁶ cycles to failure for P$_S$=97.7% equal to 225 MPa, the negative inverse slope, k, being equal to 3. The torsional calibration curve had instead $\Delta\tau_A$=160 MPa (again at N_{Ref} = 2·10⁶ cycles to failure for P$_S$=97.7%) and k₀=5. By using these

two pieces of calibration information, fatigue constants α, β, a and b in Eqs (3) and (4) were calculated to be as follows:

$$k_t(\rho_w) = -2 \cdot \rho_w + 5 \tag{21}$$

$$\Delta\tau_{Ref}(\rho_w) = -47.5\rho_w + 160 \tag{22}$$

Independently of the crack initiation location (i.e., either at toes or at roots), the log-log diagram of Fig. 7d confirms that, as expected, the FAT 225 uniaxial fatigue curves was capable of modelling the fatigue behaviour of the $\theta=0°$ welded specimens being considering not only with a remarkable level of accuracy, but also with a suitable level of conservatism.

The results obtained by applying the MWCM along with the effective notch stress approach to estimate the fatigue lifetime of the welded specimens with $\theta>0°$ are summarised in the modified Wöhler diagrams reported in Fig. 11 (see also Table 2). These charts demonstrate that the use of the MWCM along with the r_{ref} concept resulted in a very high level of accuracy, with the estimates falling within the corresponding scatter bands calculated for P_S equal to 2.3% and 97.7%. The only exception is represented by geometry BM with $\theta=43°$ (Fig. 4a) [38] for which the estimates being obtained were seen to be slightly conservative.

To conclude, it is worth observing that such a remarkable level of accuracy was reached when reanalysing not only the results characterised by weld toe failures, but also those tests where fatigue cracks were seen to initiate at the weld roots.

7. Accuracy of the MWCM applied along with the Point Method

The Theory of Critical Distances (TCD) is a theoretical framework which groups together a number of different approaches that all make use of a length scale parameter to assess fatigue strength of notched/cracked engineering materials [12, 19, 21]. The fundamental concept on which the TCD is based can be formalised in different ways that include the Point Method (PM), the Line Method (LM), the Area Method (AM), and the Volume Method (VM) [19].

Amongst these different formalisations of the same idea, certainly the PM represents the simplest way to use the TCD in situations of practical interest: this is the reason why in the present investigation the PM was preferred over the LM, the AM, and the VM. In more detail, the PM postulates that the effective stress to be used to perform fatigue assessment has to be determined at a given distance from the assumed crack initiation location. In this context, the required critical distance is seen to be a material property. In other words, for a given material, the critical distance value is not affected by the sharpness of the geometrical feature being assessed. Further, as soon as the required length scale parameter is known, the effective stresses can be determined by using a simple linear-elastic constitutive law to model the stress-strain behaviour of the material under investigation, with this holding true independently of the actual level of ductility/non-linearity that characterises the material itself [12, 21, 48].

As far as steel welded joints are concerned, to apply the MWCM along with the PM, the local-linear elastic stress components relative to the critical plane have to be determined, along the weld toe/root bisector, at a distance from the assumed crack initiation point equal to 0.5 mm [12, 29, 36] (Fig. 2b). As to this value for the PM critical distance, it is worth recalling here that it was obtained by following a fairly articulated procedure based on the use of a large amount of experimental results [29]. In particular, initially the MWCM was calibrated via the curves recommended by Eurocode 3 to design ground butt welded joints against uniaxial fatigue loading as well as against cyclic torsion. Subsequently, a unifying value for the multiaxial critical distance of 0.5 mm was estimated [12, 29] by taking full advantage of the Notch-Stress Intensity Factor (N-SIF) approach [43]. In this context, a value of 0.5 mm represents then a recommended average length that can be used without the need for calibrating the PM. However, a specific critical distance value for the particular welded metal being design can be obtained by simply following the experimental procedure as described in Ref. [12].

Turning back to the in-field usage of the MWCM applied along with the PM, as soon as the time-variable stress tensor at a distance equal to 0.5 mm from the assumed crack initiation location is known, the range of the normal stress, $\Delta\sigma_n$, as well as the range of the shear stress, $\Delta\tau$, are used to calculate stress ratio ρ_w according to definition (2). The negative inverse

slope, $k_\tau(\rho_w)$, of the corresponding modified Wöhler curve is directly derived from the following relationships [29, 36]:

$$k_\tau(\rho_w) = -2\rho_w + 5 \quad \text{for } \rho_w \leq 1 \tag{23}$$

$$k_\tau(\rho_w) = 3 \quad \text{for } \rho_w > 1 \tag{24}$$

The reference shear stress range, $\Delta\tau_{Ref}(\rho_w)$, extrapolated at $5 \cdot 10^6$ cycles to failure is instead estimated for P_S=50% from [29]:

$$\Delta\tau_{Ref}(\rho_w) = -32\rho_w + 96 \text{ [MPa]} \quad \text{for } \rho_w \leq 2 \tag{25}$$

$$\Delta\tau_{Ref}(\rho_w) = 32 \text{ [MPa]} \quad \text{for } \rho_w > 2 \tag{26}$$

and for P_S equal to 97.7% from [36]:

$$\Delta\tau_{Ref}(\rho_w) = -24\rho_w + 67 \text{ [MPa]} \quad \text{for } \rho_w \leq 2 \tag{27}$$

$$\Delta\tau_{Ref}(\rho_w) = 19 \text{ [MPa]} \quad \text{for } \rho_w > 2 \tag{28}$$

In order to check the accuracy of the MWCM applied along with the PM in estimating fatigue strength in the presence of inclined welds, the relevant linear-elastic stress states were determined, along the weld toe/root bisectors and at a distance from the crack initiation points equal to 0.5 mm, by solving three-dimensional models with FE code ANSYS®. In particular, the solutions for the different welded geometries being investigated were obtained by following a standard solid-to-solid sub-modelling procedure, with the mesh density being increased gradually until convergence occurred (see the example reported in Fig. 9).

The results obtained by applying the MWCM along with the PM are summarised in the modified Wöhler diagrams of Fig. 12 (see also Table 2). These charts demonstrate that this local stress based multiaxial fatigue assessment technique is capable of estimating the fatigue

strength of connections containing inclined welds with a remarkable level of accuracy, the advantage being that the required stress analysis can be performed by solving simple linear elastic FE models.

8. Conclusions

In the present paper the MWCM is applied along with nominal, hot-spot, and local stresses to estimate the fatigue strength of uniaxially loaded steel welded joints containing inclined welds. The accuracy and reliability of these different ways of using the MWCM to address this specific design problem were checked systematically by post-processing a large number of data taken from the technical literature. These experimental results were generated by initiating fatigue cracks not only at the weld toes, but also at the weld roots. According to the outcomes from the present research work, the most important conclusions are summarised in what follows.

- Fatigue strength of uniaxially loaded inclined welds can be assessed effectively by tackling the problem from a multiaxial fatigue angle. In particular, for this particular geometry/loading configuration, weald seams are damage by proportional multiaxial load histories, with this holding true independently of the strategy that is adopted to perform the stress analysis.

- As far as steel connections are concerned, the MWCM applied in conjunction with nominal, hot-spot, and notch stresses as well as with the TCD is seen to be highly accurate in estimating fatigue strength in the presence of uniaxially loaded inclined welds.

- Irrespective of the type of stress analysis being adopted, the MWCM's governing equations can be calibrated accurately by taking full advantage of those uniaxial and torsional reference design curves that are provided by the pertinent Standard Codes and Recommendations.

- More work needs to be done in this area to check whether this multiaxial fatigue based idea can be extended also to the fatigue assessment of uniaxially loaded aluminium joints containing inclined welds.

References

[1] Maddox SJ. Fatigue strength of welded structures. 2nd Edition, Abington Publishing, Cambridge, UK, 1991.

[2] Fricke W. Review Fatigue analysis of welded joints: state of development. Mar Struct 2003;16:185-200.

[3] Campbell F. Fatigue and Fracture: Understanding the basics, ASM International, Materials Park, OH 44073-0002, USA, 2012.

[4] Haryadi GD, Kim SJ. Influences of post weld heat treatment on fatigue crack growth behaviour of TIG welding of 6013 T4 aluminium alloy joint (part 1. Fatigue crack growth across the weld metal). J Mech Sci Technol 2011;25(9):2161-2170.

[5] Borrego LP, Costa JD, Jesus JS, Loureiro AR, Ferreira, JM. Fatigue life improvement by friction stir processing of 5083 aluminium alloy MIG butt welds. Theor Appl Fract Mec 2014;70:68-74.

[6] Schijve J. Fatigue of Structures and Materials. 2nd Edition, Springer Science & Business Media, 2009.

[7] Kimapong K, Watanabe T. Lap Joint of A5083 Aluminium Alloy and SS400 Steel by Friction Welding. Mater Trans 2005;46(4):835-841.

[8] Meco S, Pardal G, Ganguly S, Williams S, McPherson N. Application of laser in seam welding of dissimilar steel to aluminium joints for thick structural components. Opt Las Eng 2015;67:22-30.

[9] Hobbacher A. Recommendations for fatigue design of welded joints and components. IIW document XIII-2151-07/XV-1254-07; May 2007.

[10] Anon. Design of steel structures. ENV 1993-1-1, EUROCODE 3, 1988.

[11] Anon. Design of aluminium structures- Part 1-3: Structures susceptible to fatigue. EN 1999-1-3:2007/A1, EUROCODE 9, 2011.

[12] Susmel L. Multiaxial notch fatigue: from nominal to local stress–strain quantities. Woodhead Publishing Limited, Cambridge, UK, 2009.

[13] Radaj D, Sonsino CM, Fricke W. Fatigue assessment of welded joints by local approaches. Woodhead Publishing Limited, Cambridge, UK, 2007.

[14] Niemi E, Fricke W, Maddox SJ. Fatigue Analysis of Welded Components: Designer's Guide to the Structural Hot-Spot Stress Approach, Woodhead Publishing Limited, Cambridge, UK, 2006.

[15] Fricke W, Sonsino CM. Notch stress concepts for the fatigue assessment of welded Joints- Background and applications. Int J Fatigue 2012;34:2-16.

[16] Morgenstern C, Sonsino CM, Hobbacher A, Sorbo F. Fatigue design of aluminium welded joints by the local stress concep with the ficitious notch radius of r_f=1 mm. Int J Fatigue 2006;28:881-890.

[17] Karakas O, Morgenstern C, Sonsino CM. Fatigue design of welded joints from the wrought magnesium alloy AZ31 by the local stress concept with the fictitious notch radii of r_f=1.0 and 0.05 mm. Int J Fatigue 2008;30:2210-2219.

[18] Sonsino CM. A consideration of allowable equivalent stresses for fatigue design of welded joints according to the notch stress concept with the reference radii r_{ref} = 1.00 and 0.05 mm. Weld World 2009;53(3/4):R64–75.

[19] Taylor D. Geometrical effects in fatigue: a unifying theoretical model. Int J Fatigue 1999;21:413-420.

[20] Taylor D, Barrett N, Lucano G. Some new methods for predicting fatigue in welded joints. Int J Fatigue 2002;24:509–18.

[21] Taylor D. The Theory of Critical Distances: a new perspective in Fracture Mechanics. Elsevier, Oxford, UK, 2007.

[22] Susmel L. Nominal stresses and Modified Wöhler Curve Method to perform the fatigue assessment of uniaxially-loaded inclined welds. P I Mech Eng C-J Mec 2014;228(16):2871-2880.

[23] Susmel L, Lazzarin P. A Bi-Parametric Modified Wöhler Curve for High Cycle Multiaxial Fatigue Assessment. Fatigue Fract Engng Mater Struct 2002;25:63-78.

[24] Lazzarin P, Susmel L. A Stress-Based Method to Predict Lifetime under Multiaxial Fatigue Loadings. Fatigue Fract Engng Mater Struct 2003;26:1171-1187.

[25] Susmel L. Multiaxial Fatigue Limits and Material Sensitivity to Non-Zero Mean Stresses Normal to the Critical Planes. Fatigue Fract Engng Mater Struct 2008;31:295-309.

[26] Susmel L, Tovo R, Lazzarin P. The mean stress effect on the high-cycle fatigue strength from a multiaxial fatigue point of view. Int J Fatigue 2005;27:928-943.

[27] Susmel L, Tovo R. On the use of nominal stresses to predict the fatigue strength of welded joints under biaxial cyclic loading. Fatigue Fract Eng Mater Struct 2004;27:1008-1024.

[28] Susmel L, Tovo R. Local and structural multiaxial stress states in welded joints under fatigue loading. Int J Fatigue 2006;28:564-575.

[29] Susmel L. Modified Wöhler Curve Method, Theory of Critical Distances and EUROCODE 3: a novel engineering procedure to predict the lifetime of steel welded joints subjected to both uniaxial and multiaxial fatigue loading. Int J Fatigue 2008;30:888-907.

[30] Susmel L, Tovo R, Benasciutti D. A novel engineering method based on the critical plane concept to estimate the lifetime of weldments subjected to variable amplitude multiaxial fatigue loading. Fatigue Fract Engng Mater Struct 2009;32:441–459.

[31] Susmel L. The Modified Wöhler Curve Method calibrated by using standard fatigue curves and applied in conjunction with the Theory of Critical Distances to estimate fatigue lifetime of aluminium weldments. Int J Fatigue 2009;31:197-212.

[32] Susmel L. Three different ways of using the Modified Wöhler Curve Method to perform the multiaxial fatigue assessment of steel and aluminium welded joints. Eng Fail Anal 2009;16:1074–1089.

[33] Susmel L. Estimating fatigue lifetime of steel weldments locally damaged by variable amplitude multiaxial stress fields. Int J Fatigue 2010;32:1057–1080.

[34] Susmel L, Sonsino CM, Tovo R. Accuracy of the Modified Wöhler Curve Method applied along with the r_{ref}=1 mm concept in estimating lifetime of welded joints subjected to multiaxial fatigue loading. Int J Fatigue 2011;33:1075-1091.

[35] Susmel L, Askes H. Modified Wöhler Curve Method and multiaxial fatigue assessment of thin welded joints. Int J Fatigue 2012;43:30–42.

[36] Susmel L. Four stress analysis strategies to use the Modified Wöhler Curve Method to perform the fatigue assessment of weldments subjected to constant and variable amplitude multiaxial fatigue loading. Int J Fatigue 2014;64:38-54.

[37] Susmel L. A simple and efficient numerical algorithm to determine the orientation of the critical plane in multiaxial fatigue problems. Int J Fatigue 2010;32:1875–1883.

[38] Booth GS, Maddox SJ. Influence of various factors on the fatigue strength of steel plates with fillet welded attachments. TWI Research Report no. 93, Cambridge, UK, 1979.

[39] Kim I-T, Kainuma S. Fatigue life assessment of load-carrying fillet welded cruciform joints inclined to uniaxial cyclic loading. Int J Pres Ves Pip 2005;82:807-813.

[40] Kim I-T, Yamada K. Fatigue behaviour of fillet welded joints inclined to a uniaxial cyclic load. IIW Document XIII-2021-04, 2004.

[41] Maddox SJ. Fatigue assessment of welds not oriented either normal or parallel to the direction of loading. IIW Document JWG XIII/XV-218-10, 2010.

[42] Lazzarin P, Tovo R. A unified approach to the evaluation of linear elastic stress fields in the neighbourhood of cracks and notches. Int J Fracture 1996;78:3–19.

[43] Lazzarin P, Tovo R. A notch intensity factor approach to the stress analysis of welds. Fatigue Fract Engng Mater Struct 1998;21:1089-1103.

[44] Lazzarin P, Sonsino CM, Zambardi R. A notch stress intensity approach to assess the multiaxial fatigue strength of welded tube-to-flange joints subjected to combined loadings. Fatigue Fract Eng Mater Struct 2004; 27: 127–140.

[45] Haibach E. Service fatigue-strength – methods and data for structural analysis. VDI, Düsseldorf, Germany 1992.

[46] Radaj D, Sonsino CM, Fricke W. Recent developments in local concepts of fatigue assessment of welded joints. Int J Fatigue 2009;31:2-11.

[47] Radaj D. Design and analysis of fatigue resistant welded structures. Woodhead Publishing Limited, Cambridge, UK, 1990.

[48] Santus C, Taylor D, Benedetti M. Experimental determination and sensitivity analysis of the fatigue critical distance obtained with rounded V-notched specimens. Int J Fatigue 2018;113;113-125.

List of Captions

Tables

Table 1 (<u>continued on the next page</u>). Experimental data and stress components relative to the critical plane calculated in terms of nominal stresses and hot-spot stresses.

Code	θ	$\Delta\sigma_{nom}$	N_f (·10³) [Cycles to Failure]	Nominal Stress			Hot-spot stress			Comment
				$\Delta\tau$ [MPa]	$\Delta\sigma_n$ [MPa]	ρ_w	$\Delta\tau$ [MPa]	$\Delta\sigma_n$ [MPa]	ρ_w	
BM0-01	0	240	134	119.6	119.6		129.0	126.8		
BM0-02	0	200	240	99.8	99.8		107.6	105.8		
BM0-03	0	160	281	79.6	79.6	1.000	85.8	84.4	0.983	
BM0-04	0	140	787	69.9	69.9		75.4	74.2		
BM0-05	0	120	1667	59.8	59.8		64.6	63.4		
BM0-06	0	100	2728	49.9	49.9		53.8	53.0		
BM31-01	31	260	181	149.1	95.4		216.4	173.2		
BM31-02	31	200	554	114.6	73.3		166.4	133.2		
BM31-03	31	160	950	91.7	58.6	0.640	133.0	106.4	0.800	
BM31-04	31	120	1848	68.9	44.0		100.0	80.0		
BM31-05	31	110	2872	63.3	40.5		91.8	73.6		
BM31-06	31	90	6170	51.2	32.7		74.2	59.4		Run Out
BM43-01	43	260	268	147.4	69.6		244.2	155.4		
BM43-02	43	200	684	113.6	53.7		188.2	119.8		
BM43-03	43	160	1306	90.6	42.8	0.473	150.0	95.4	0.637	
BM43-04	43	130	2040	73.5	34.7		121.6	77.4		
BM43-05	43	115	3806	65.2	30.8		108.0	68.8		
BM43-06	43	100	5887	56.9	26.9		94.4	60.0		Run Out
KK-0-01	0	111	158	55.4	55.4		-	-	-	
KK-0-02	0	77	466	38.6	38.6		-	-	-	
KK-0-03	0	56	1740	28.2	28.2	1.000	-	-	-	
KK-0-04	0	55	2250	27.7	27.7		-	-	-	
KK-0-05	0	36	3100	18.2	18.2		-	-	-	
KK-0-06	0	26	19200	13.1	13.1		-	-	-	
KK-15-01	15	103	270	58.2	51.3		-	-	-	
KK-15-02	15	72	756	41.1	36.2		-	-	-	
KK-15-03	15	54	2060	30.7	27.1	0.881	-	-	-	
KK-15-04	15	33	10900	18.7	16.5		-	-	-	
KK-15-05	15	29	15700	16.3	14.4		-	-	-	
KK-30-01	30	83	664	63.0	41.3		-	-	-	
KK-30-02	30	55	1980	41.9	27.4	0.655	-	-	-	
KK-30-03	30	42	6010	32.3	21.1		-	-	-	
KK-30-04	30	30	19000	23.2	15.2		-	-	-	
KK-45-01	45	60	2160	66.5	29.8		-	-	-	
KK-45-02	45	54	2360	60.4	27.0	0.447	-	-	-	
KK-45-03	45	48	3030	53.3	23.9		-	-	-	
KK-45-04	45	28	18200	30.6	13.7		-	-	-	

KY-G-0-01	0	190	216	95.0	95.0		102.3	101.9		
KY-G-0-02	0	190	237	95.0	95.0	1.000	102.3	101.9	0.996	
KY-G-0-03	0	120	1564	60.0	60.0		64.6	64.3		
KY-G-0-04	0	98	3428	49.0	49.0		52.8	52.6		
KY-G-45-01	45	190	394	106.2	47.5		135.1	62.7		
KY-G-45-02	45	190	702	106.2	47.5		135.1	62.7		
KY-G-45-03	45	152	623	85.0	38.0		108.1	50.2		
KY-G-45-04	45	152	1200	85.0	38.0		108.1	50.2		
KY-G-45-05	45	190	1447	106.2	47.5	0.447	135.1	62.7	0.464	
KY-G-45-06	45	204	735	114.0	51.0		145.0	67.3		
KY-G-45-07	45	190	1278	106.2	47.5		135.1	62.7		
KY-G-45-08	45	190	982	106.2	47.5		135.1	62.7		
KY-G-45-09	45	152	2270	85.0	38.0		108.1	50.2		Run Out
KY-N-0-01	0	206	198	103.0	103.0		120.2	120.2		
KY-N-0-02	0	203	170	101.5	101.5		118.5	118.5		
KY-N-0-03	0	160	470	80.0	80.0		93.4	93.4		
KY-N-0-04	0	160	556	80.0	80.0		93.4	93.4		
KY-N-0-05	0	136	1415	68.0	68.0	1.000	79.4	79.4	1.000	
KY-N-0-06	0	136	630	68.0	68.0		79.4	79.4		
KY-N-0-07	0	136	990	68.0	68.0		79.4	79.4		
KY-N-0-08	0	113	2788	56.5	56.5		66.0	66.0		
KY-N-0-09	0	113	6764	56.5	56.5		66.0	66.0		Run Out
KY-N-15-01	15	206	360	109.0	96.1		127.1	105.3		
KY-N-15-02	15	203	324	107.4	94.7		125.3	103.7		
KY-N-15-03	15	161	479	85.2	75.1		99.3	82.3		
KY-N-15-04	15	160	867	84.7	74.6		98.7	81.8		
KY-N-15-05	15	160	760	84.7	74.6		98.7	81.8		
KY-N-15-06	15	136	1577	72.0	63.4	0.881	83.9	69.5	0.828	
KY-N-15-07	15	136	1739	72.0	63.4		83.9	69.5		
KY-N-15-08	15	136	984	72.0	63.4		83.9	69.5		
KY-N-15-09	15	123	2366	65.1	57.4		75.9	62.8		
KY-N-15-10	15	123	4860	65.1	57.4		75.9	62.8		Run Out
KY-N-30-01	30	206	502	118.0	77.3		116.4	76.2		
KY-N-30-02	30	203	389	116.3	76.1		118.2	77.4		
KY-N-30-03	30	174	1264	99.7	65.3		108.8	71.2		
KY-N-30-04	30	159	2053	91.1	59.6		99.4	65.2		
KY-N-30-05	30	159	1620	91.1	59.6	0.655	91.2	59.8	0.655	
KY-N-30-06	30	138	6449	79.0	51.8		91.2	59.8		
KY-N-30-07	30	138	10000	79.0	51.8		79.0	51.8		Run Out
KY-N-30-08	30	123	10000	70.5	46.1		79.0	51.8		Run Out

Table 2 (continued on the next page). Experimental data and stress components relative to the critical plane calculated in terms of effective notch stresses and the Point Method.

Code	θ	$\Delta\sigma_{nom}$	N_f (·10³) [cycles to failure]	Effective notch stress			Point Method			Comment
				$\Delta\tau$ [MPa]	$\Delta\sigma_n$ [MPa]	ρ_w	$\Delta\tau$ [MPa]	$\Delta\sigma_n$ [MPa]	ρ_w	
BM0-01	0	240	134	410.0	409.6		204.4	235.8		
BM0-02	0	200	240	342.2	341.8		170.5	196.7		
BM0-03	0	160	281	273.0	272.6	0.999	136.0	156.9	1.154	
BM0-04	0	140	787	239.6	239.4		119.4	137.7		
BM0-05	0	120	1667	205.0	204.8		102.2	117.9		
BM0-06	0	100	2728	171.0	170.8		85.2	98.3		
BM31-01	31	260	181	523.6	482.2		233.8	238.8		
BM31-02	31	200	554	402.6	370.6		179.8	183.6		
BM31-03	31	160	950	321.8	296.4	0.921	143.8	146.8	1.021	
BM31-04	31	120	1848	242.0	222.8		108.0	110.4		
BM31-05	31	110	2872	222.2	204.6		99.2	101.4		
BM31-06	31	90	6170	179.4	165.2		80.2	81.8		Run Out
BM43-01	43	260	268	663.0	604.2		257.2	258.6		
BM43-02	43	200	684	511.2	466.0		198.2	199.4		
BM43-03	43	160	1306	407.5	371.4	0.912	158.0	158.8	1.006	
BM43-04	43	130	2040	330.4	301.2		128.2	129.0		
BM43-05	43	115	3806	293.2	267.4		113.8	114.4		
BM43-06	43	100	5887	256.2	233.4		99.4	100.0		Run Out
KK-0-01	0	111	158	302.0	654.2		84.0	176.7		
KK-0-02	0	77	466	209.5	453.8		58.5	123.1		
KK-0-03	0	56	1740	152.4	330.1	2.166	42.8	90.0	2.103	
KK-0-04	0	55	2250	149.6	324.2		42.1	88.4		
KK-0-05	0	36	3100	98.0	212.2		27.6	58.0		
KK-0-06	0	26	19200	70.7	153.2		19.9	41.9		Run Out
KK-15-01	15	103	270	305.4	316.3		107.3	142.6		
KK-15-02	15	72	756	213.5	221.1		75.7	100.5		
KK-15-03	15	54	2060	160.1	165.8	1.036	56.6	75.2	1.328	
KK-15-04	15	33	10900	97.9	101.3		34.4	45.8		
KK-15-05	15	29	15700	86.0	89.1		30.1	39.9		
KK-30-01	30	83	664	212.5	219.7		96.6	99.9		
KK-30-02	30	55	1980	140.8	145.6	1.034	64.2	66.4	1.034	
KK-30-03	30	42	6010	107.5	111.2		49.5	51.2		
KK-30-04	30	30	19000	76.8	79.4		35.6	36.8		Run Out
KK-45-01	45	60	2160	121.6	128.9		105.4	105.8		
KK-45-02	45	54	2360	109.5	116.0	1.060	95.7	96.0	1.004	
KK-45-03	45	48	3030	97.3	103.1		84.5	84.8		
KK-45-04	45	28	18200	56.8	60.1		48.4	48.6		Run Out

KY-G-0-01	0	190	216	258.7	256.7		221.8	305.3		
KY-G-0-02	0	190	237	258.7	256.7	0.992	221.8	305.3	1.376	
KY-G-0-03	0	120	1564	163.4	162.1		140.1	192.8		
KY-G-0-04	0	98	3428	133.4	132.4		114.4	157.5		
KY-G-45-01	45	190	394	253.1	254.0		296.5	387.1		
KY-G-45-02	45	190	702	253.1	254.0		296.5	387.1		
KY-G-45-03	45	152	623	202.5	203.2		237.2	309.6		
KY-G-45-04	45	152	1200	202.5	203.2		237.2	309.6		
KY-G-45-05	45	190	1447	253.1	254.0	1.004	296.5	387.1	1.305	
KY-G-45-06	45	204	735	271.7	272.7		318.4	415.6		
KY-G-45-07	45	190	1278	253.1	254.0		296.5	387.1		
KY-G-45-08	45	190	982	253.1	254.0		296.5	387.1		
KY-G-45-09	45	152	2270	253.1	254.0		237.2	309.6		Run Out
KY-N-0-01	0	206	198	265.4	325.4		227.1	310.1		
KY-N-0-02	0	203	170	269.5	330.5		223.8	305.6		
KY-N-0-03	0	160	470	248.0	304.1		176.4	240.9		
KY-N-0-04	0	160	556	248.0	304.1		176.4	240.9		
KY-N-0-05	0	136	1415	208.7	255.9	1.226	149.9	204.7	1.366	
KY-N-0-06	0	136	630	209.4	256.7		149.9	204.7		
KY-N-0-07	0	136	990	177.3	217.4		149.9	204.7		
KY-N-0-08	0	113	2788	177.9	218.1		124.6	170.1		
KY-N-0-09	0	113	6764	157.3	192.8		124.6	170.1		Run Out
KY-N-15-01	15	206	360	244.6	245.0		249.8	299.2		
KY-N-15-02	15	203	324	248.4	248.8		246.1	294.8		
KY-N-15-03	15	161	479	228.6	229.0		195.2	233.8		
KY-N-15-04	15	160	867	228.6	229.0		194.0	232.4		
KY-N-15-05	15	160	760	192.4	192.7	1.002	194.0	232.4	1.199	
KY-N-15-06	15	136	1577	193.0	193.3		164.9	197.5		
KY-N-15-07	15	136	1739	163.4	163.7		164.9	197.5		
KY-N-15-08	15	136	984	163.9	164.2		164.9	197.5		
KY-N-15-09	15	123	2366	144.9	145.2		149.1	178.6		
KY-N-15-10	15	123	4860	136.3	136.5		149.1	178.6		Run Out
KY-N-30-01	30	206	502	274.4	273.0		262.7	252.6		
KY-N-30-02	30	203	389	278.7	277.2		258.9	248.9		
KY-N-30-03	30	174	1264	256.4	255.1		221.9	213.4		
KY-N-30-04	30	159	2053	256.4	255.1	0.995	202.8	195.0	0.965	
KY-N-30-05	30	159	1620	215.8	214.7		202.8	195.0		
KY-N-30-06	30	138	6449	216.5	215.4		176.0	169.2		
KY-N-30-07	30	138	10000	183.3	182.4		176.0	169.2		Run Out
KY-N-30-08	30	123	10000	183.9	183.0		156.9	150.8		Run Out

Figures

(a) Nominal stress approach

(b) Hot-spot stress approach

$$\Delta\sigma_{HS} = 1.67 \cdot \Delta\sigma_{0.4t} - 0.67 \cdot \Delta\sigma_t$$
$$\Delta\tau_{HS} = 1.67 \cdot \Delta\tau_{0.4t} - 0.67 \cdot \Delta\tau_t$$

Normal Stress

$\Delta\sigma_{HS}$

Stress normal to the weld

o 0.4t t Distance

$\Delta\tau_{HS}$

Shear Stress

Shear stress parallel to the weld

Stress distribution

z

y o x

Nominal Section

z

y o x

Distance

$$[\Delta\sigma] = \begin{bmatrix} \Delta\sigma_x & \Delta\tau_{xy} & 0 \\ \Delta\tau_{xy} & 0 & 0 \\ 0 & 0 & 0 \end{bmatrix} \text{Nominal stresses}$$

$$[\Delta\sigma] = \begin{bmatrix} \Delta\sigma_x & \Delta\tau_{xy} & 0 \\ \Delta\tau_{xy} & 0 & 0 \\ 0 & 0 & 0 \end{bmatrix} \text{Hot-spot stresses}$$

(c)

$(\Delta\tau, \Delta\sigma_n, \rho_w)$

$\Delta\tau$

$\Delta\tau$

$\Delta\tau_{Ref}(\rho_w)$

$\dfrac{1}{k_\tau(\rho_w)}$

$(\Delta\tau_{Ref}(\rho_w), k_\tau(\rho_w))$

N_f N_{Ref} Cycles to failure

Figure 1. The MWCM to estimate fatigue lifetime of welded components applied in terms of nominal and hot-spot stresses.
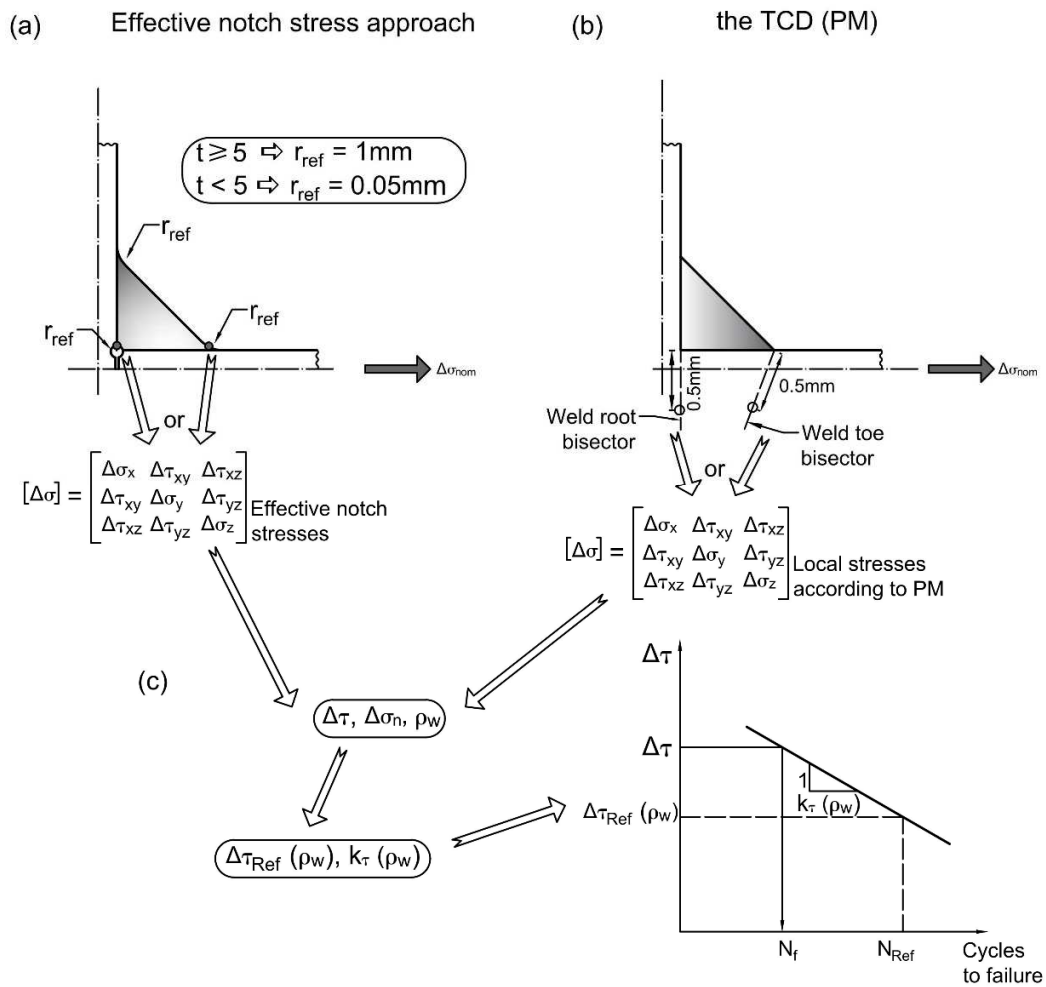
Figure 2. The MWCM to estimate fatigue lifetime of welded components applied in terms of effective notch stress as well as along with the PM.
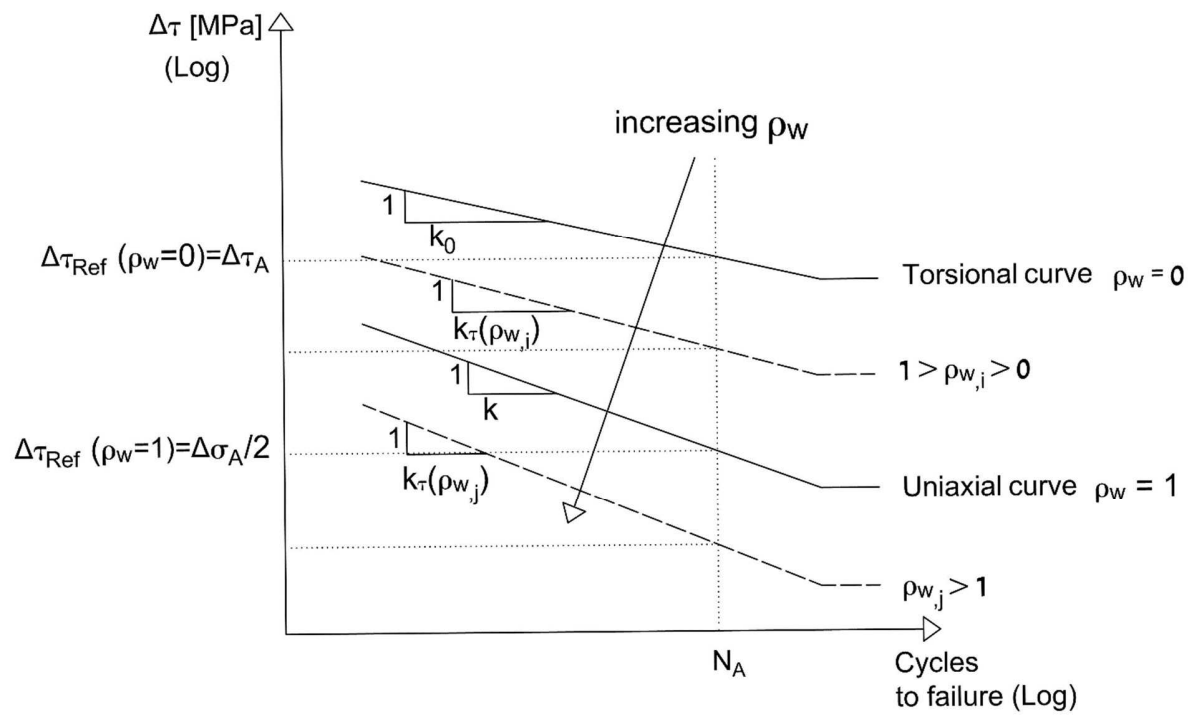
Figure 3. Modified Wöhler diagram.
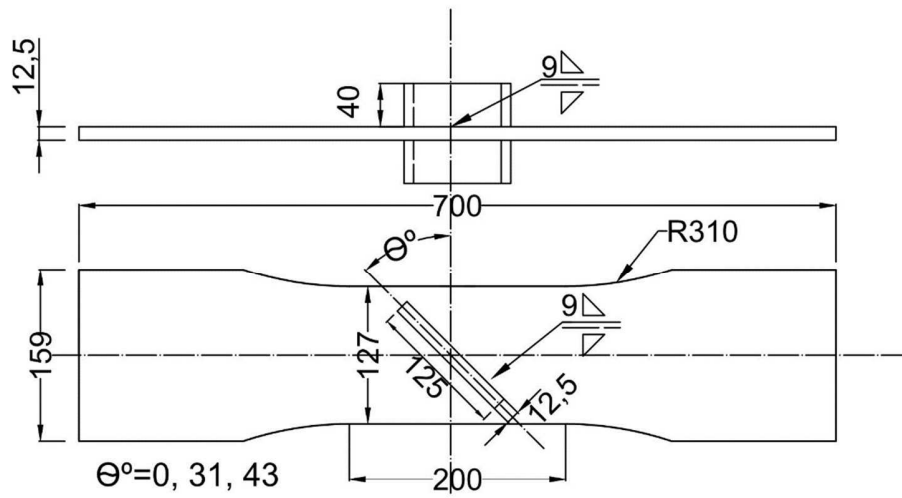
(a) Welded Specimen BM
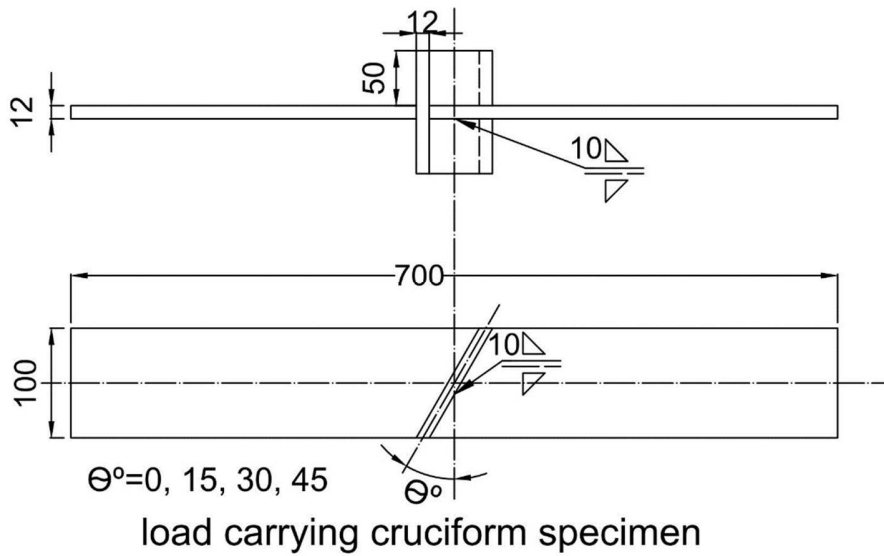
(b) Welded Specimen KK

Figure 4. Fatigue specimens tested by Booth and Maddox [38] (a) and load carrying cruciform specimens tested by Kim and Kainuma [39] (b).
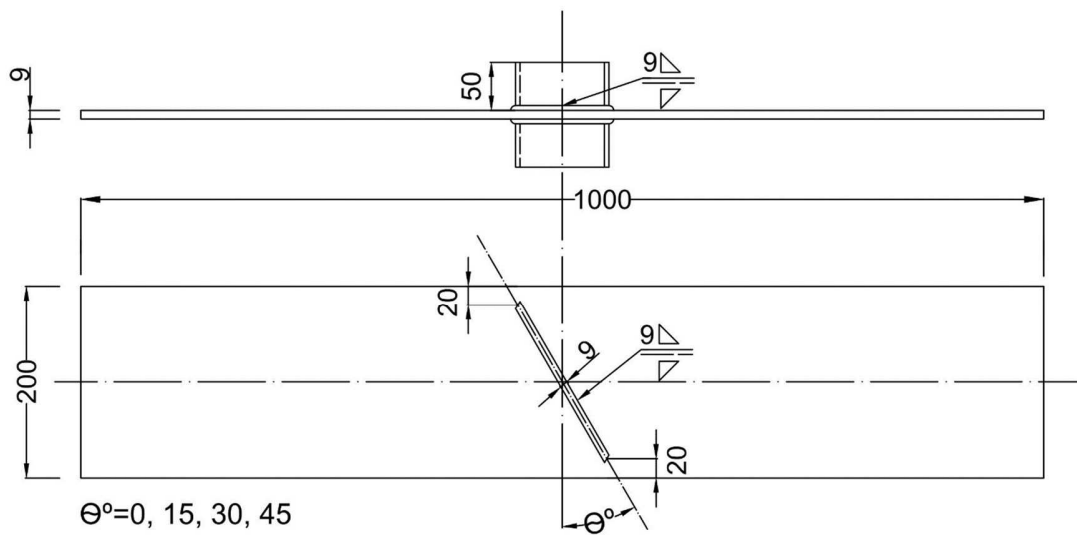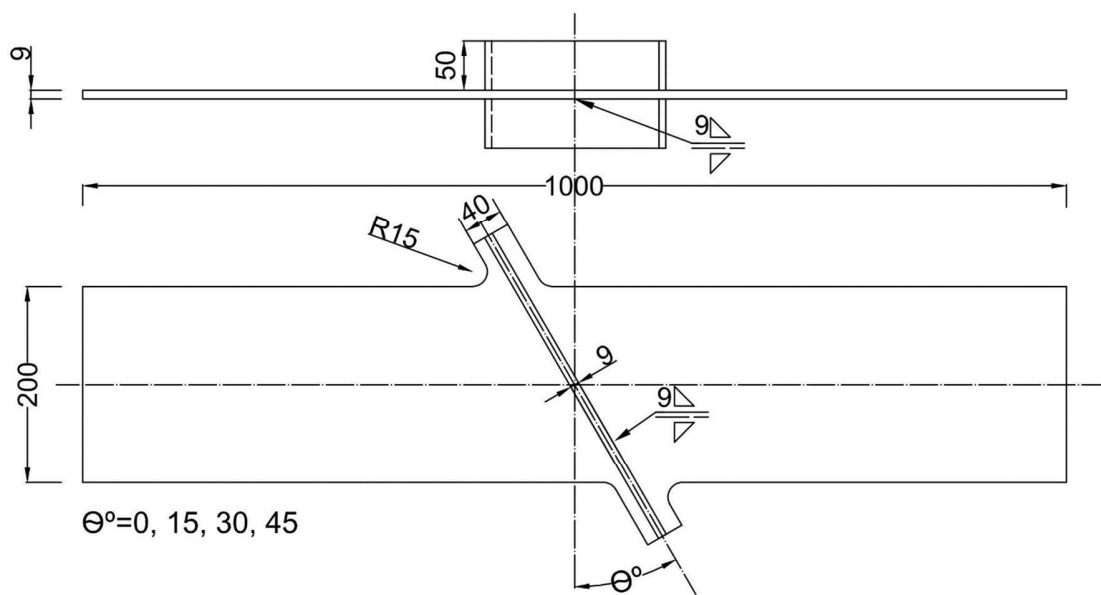
(a) Welded Specimen KY-G

(b) Welded Specimen KY-N

Figure 5. Out-of-plane gusset specimens (a) and non-load carrying cruciform specimens (b) tested by Kim and Yamada [40].
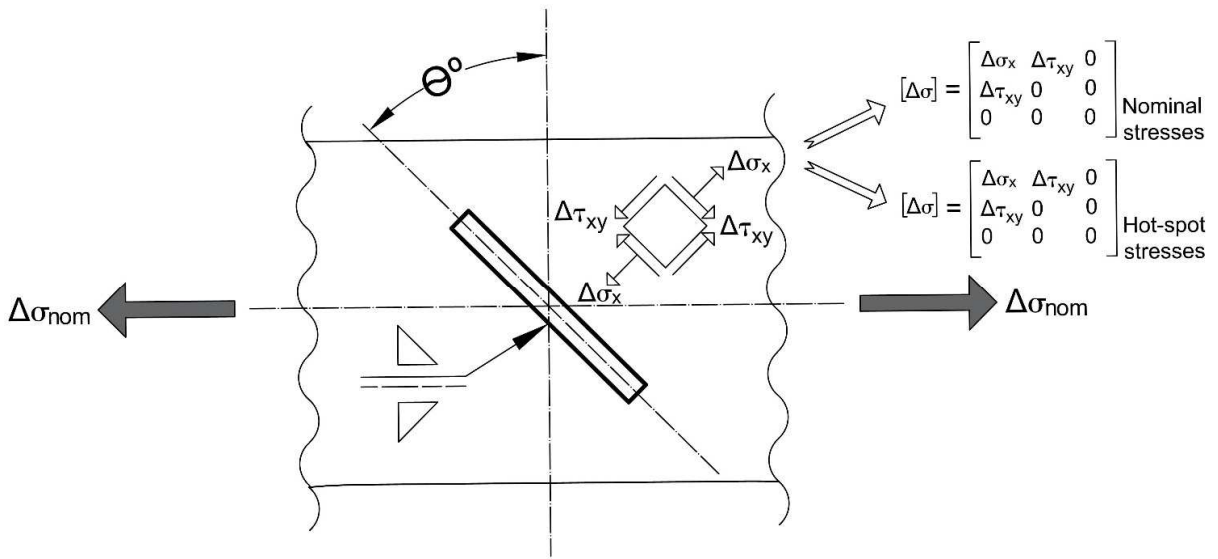
(a)
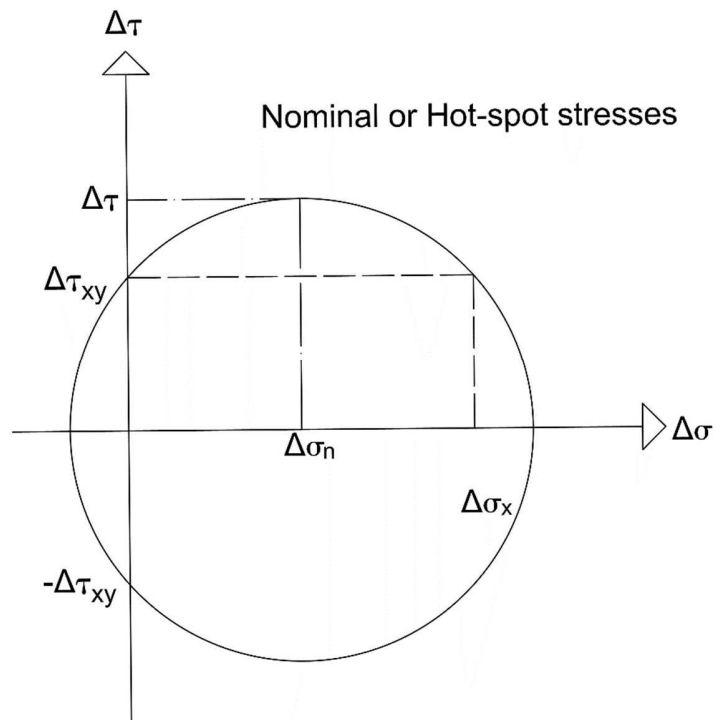
(b)

Figure 6. Nominal and hot-spot stresses in inclined welded joints subjected to uniaxial cyclic loading (a); Mohr's circle to calculate the stress components relative to the critical plane (b).
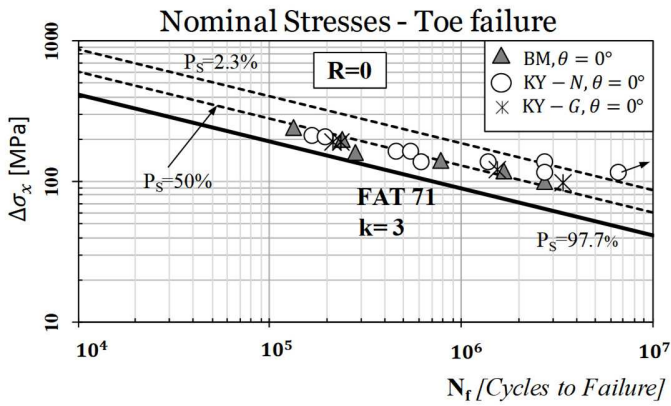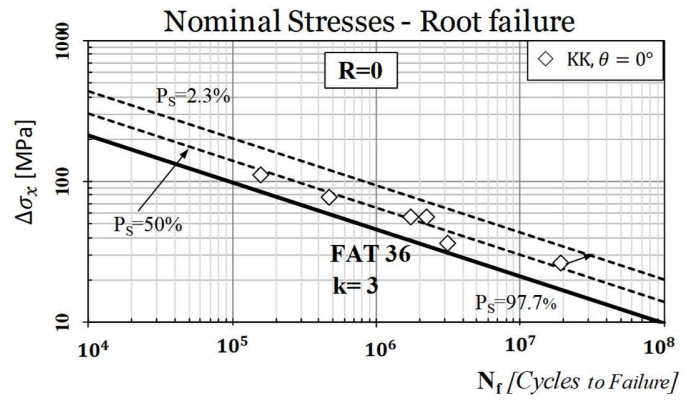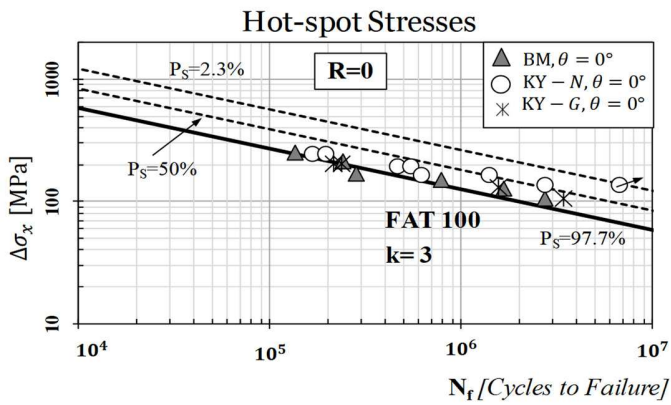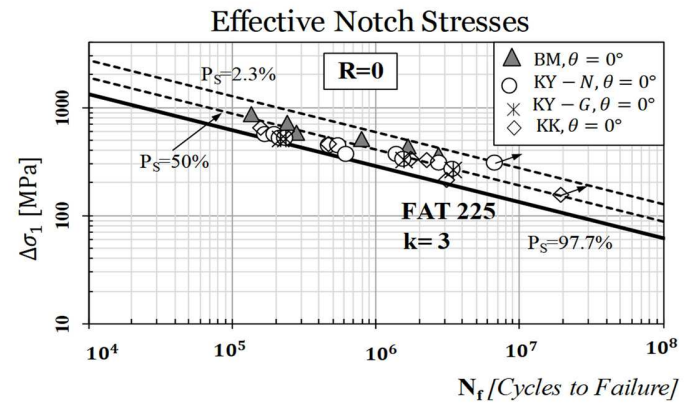
Figure 7. Accuracy of the recommended reference design curves in estimating the fatigue strength of the investigated welded joints in terms of nominal stresses.
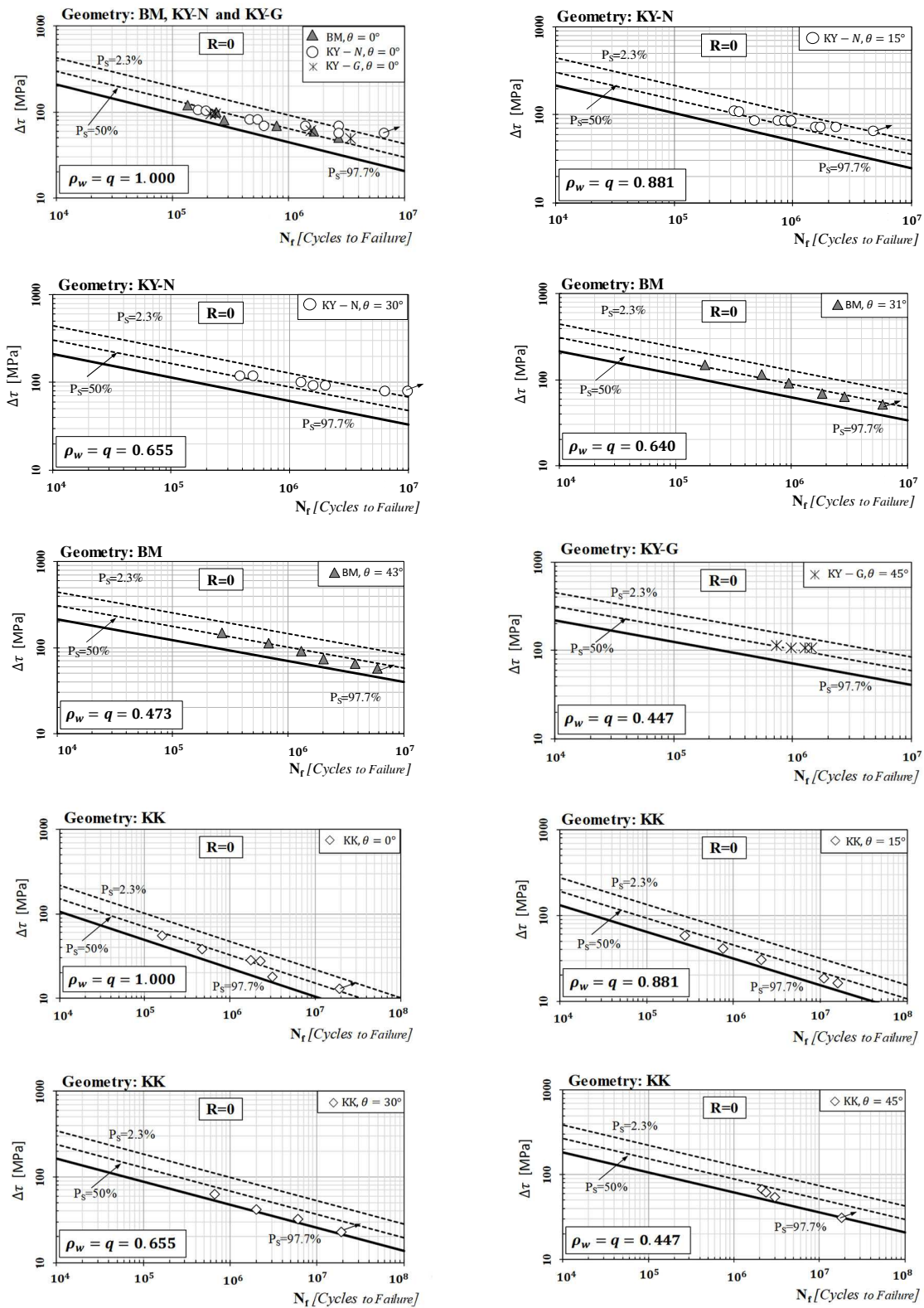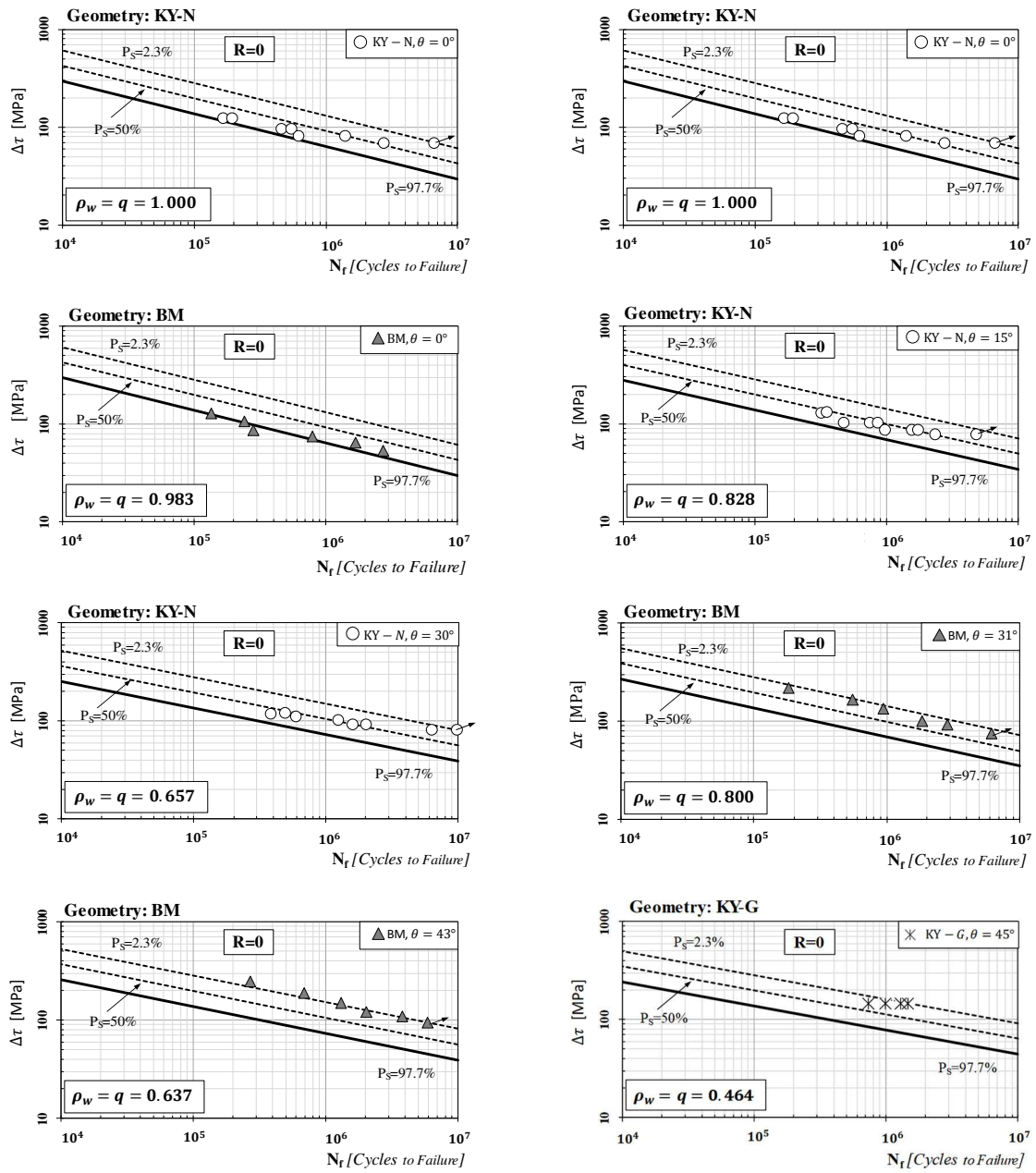
Figure 8. Accuracy of the MWCM applied along with nominal stresses in estimating fatigue strength in the presence of inclined welds.
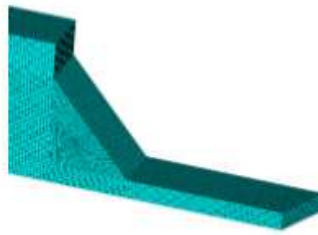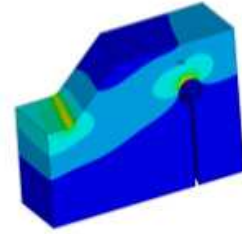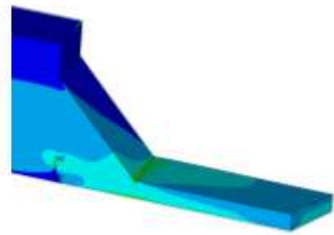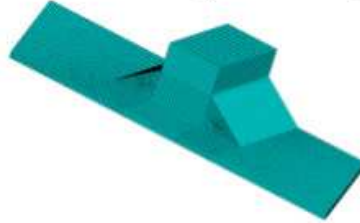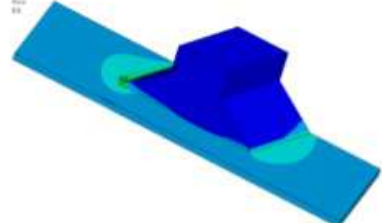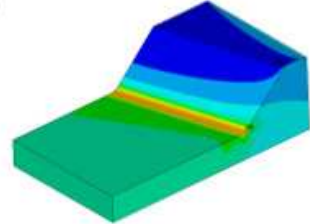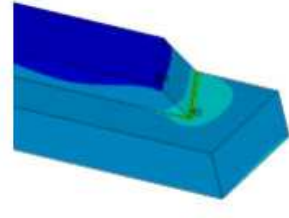
Figure 9. Examples of the linear-elastic FE models solved by following a solid-to-solid sub-modelling procedure.

Figure 10. Accuracy of the MWCM applied along with hot-spot stresses in estimating fatigue strength in the presence of inclined welds.
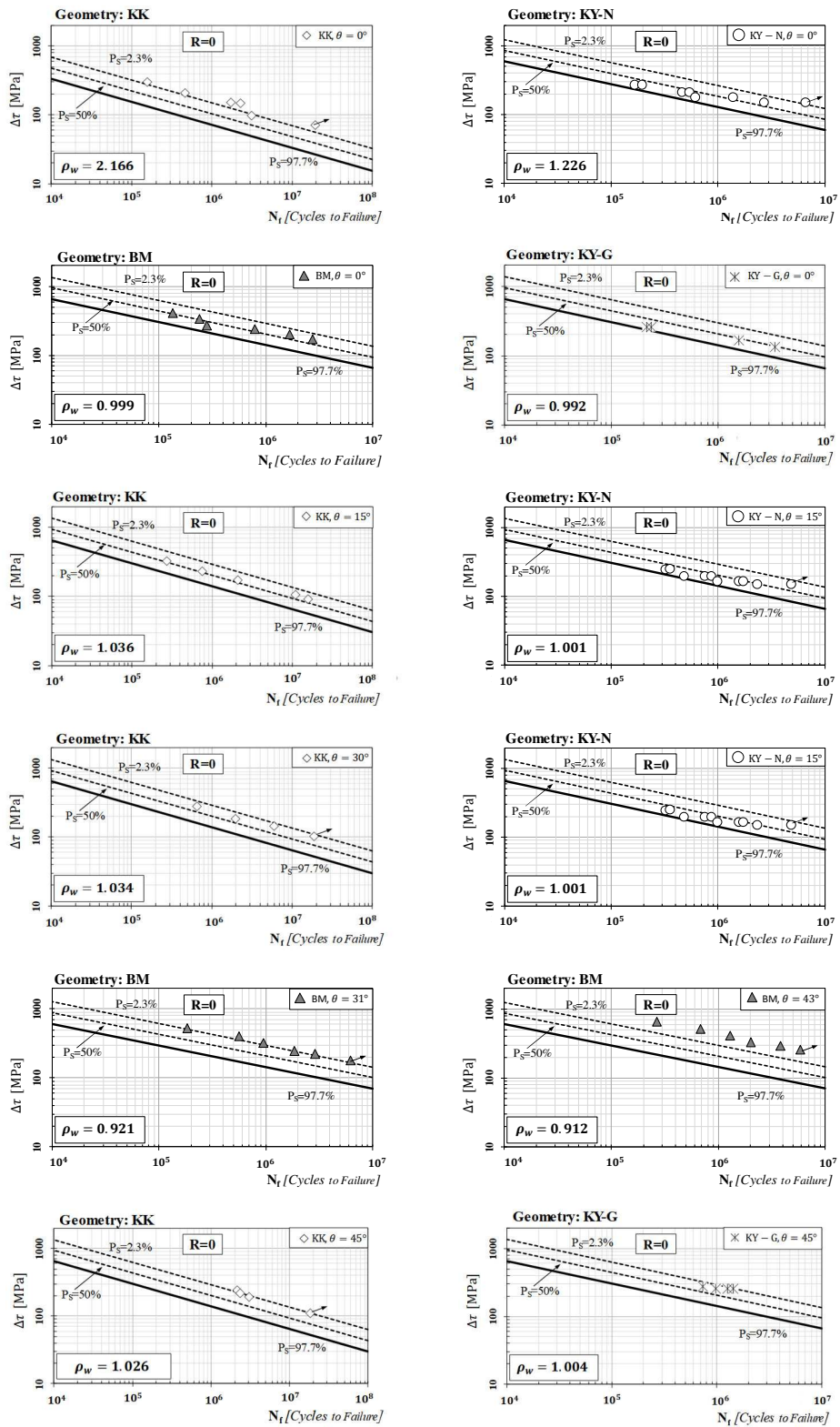
Figure 11. Accuracy of the MWCM applied along with effective notch stresses in estimating fatigue strength in the presence of inclined welds.
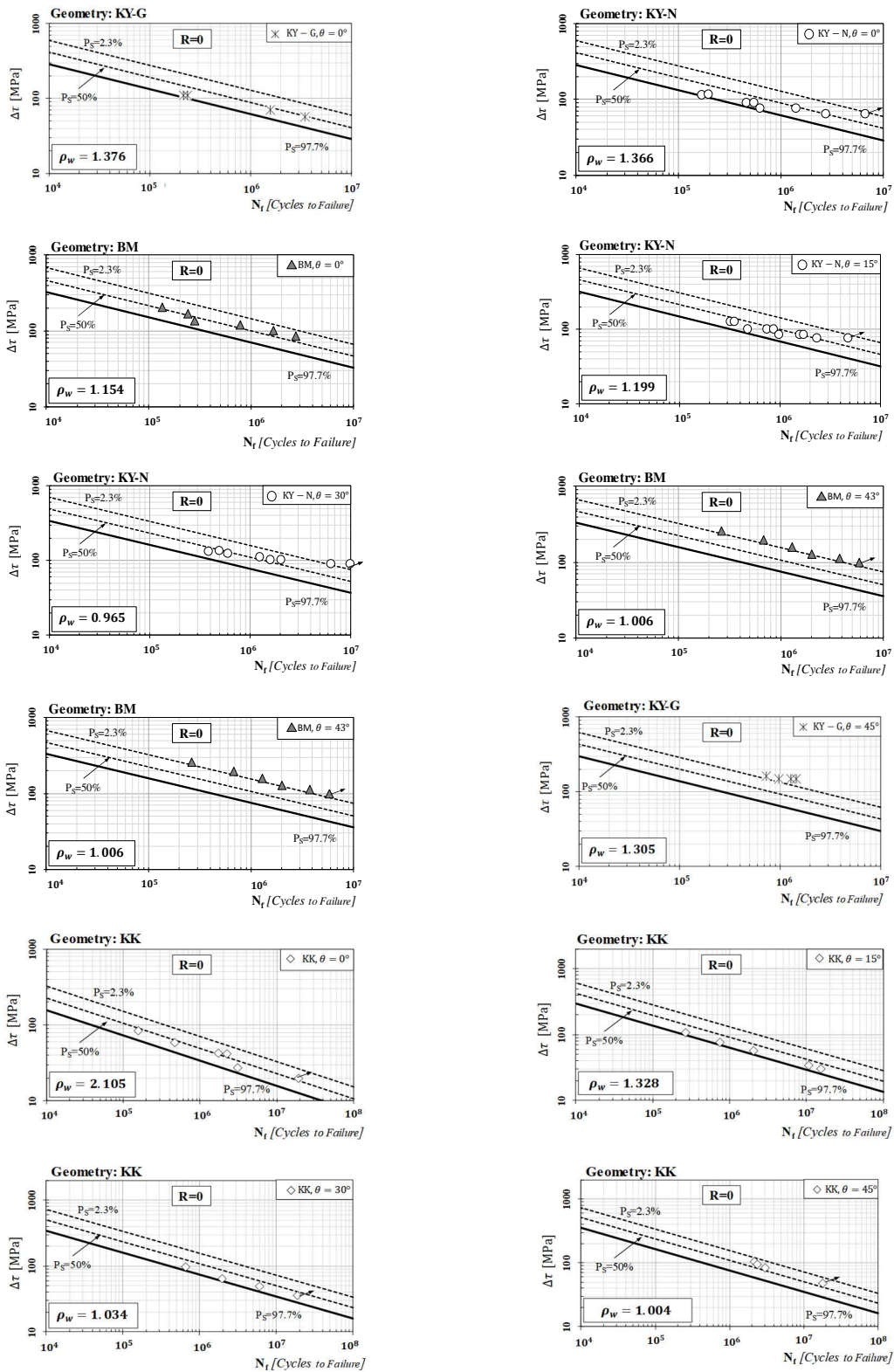
Figure 12. Accuracy of the MWCM applied along with the PM in estimating fatigue strength in the presence of inclined welds.